Schwank, M., Grant, J. P., Saleh, K., Van de Griend, A. A., Wigneron, J.-P., Guglielmetti, M., Kerr, Y., Skou, N. (2008): Calibration of the L-MEB Model over a Coniferous and a Deciduous Forest. - IEEE Transactions on Geoscience and Remote Sensing, 46, 3, 808-818

DOI: 10.1109/TGRS.2007.914801

Calibration of the L-MEB Model Over a Coniferous and a Deciduous Forest

Jennifer P. Grant, Kauzar Saleh-Contell, Jean-Pierre Wigneron, *Senior Member, IEEE*, Massimo Guglielmetti, Yann H. Kerr, *Senior Member, IEEE*, Mike Schwank, Niels Skou, *Fellow, IEEE*, and Adriaan A. Van de Griend

***Abstract*—In this paper, the L-band Microwave Emission of the Biosphere (L-MEB) model used in the Soil Moisture and Ocean Salinity (SMOS) Level 2 Soil Moisture algorithm is calibrated using L-band (1.4 GHz) microwave measurements over a coniferous (Pine) and a deciduous (mixed/Beech) forest. This resulted in working values of the main canopy parameters optical depth (τ), single scattering albedo (ω), and structural parameters $tt(\mathrm{H})$ and $tt(\mathrm{V})$, besides the soil roughness parameters H_{R} and N_{R}. Using these calibrated values in the forward model resulted in a root mean-square error in brightness temperatures from 2.8 to 3.8 K, depending on data set and polarization. Furthermore, the relationship between canopy optical depth and leaf area index is investigated for the deciduous site. Finally, a sensitivity study is conducted for the focus parameters, temperature, soil moisture, and precipitation. The results found in this paper will be integrated in the operational SMOS Level 2 Soil Moisture algorithm and used in future inversions of the L-MEB model, for soil moisture retrievals over heterogeneous, partly forested areas.**

***Index Terms*—Forest, L-band, microwave radiometry, soil moisture, Soil Moisture and Ocean Salinity (SMOS).**

I. Introduction

THE ACCURACY of radiometric (e.g., L-band or 1.4 GHz) soil moisture retrievals over vegetated land surfaces depends to a great amount on the properties of the vegetation layer. A vegetation layer covering the soil scatters and attenuates soil emission and will add its own emission to the total radiation measured above the canopy. This effect was modeled by Kirdyashev *et al.* [1]. The thicker or denser this layer, or the higher the frequency of measurement, the smaller the influence of the soil signal on the total above-canopy emission. Obviously, soil moisture retrievals will be less accurate over dense forests than over sparse vegetation. Previous microwave forest studies were therefore generally done at higher frequencies than L-band, focusing on the measurement of forest biometric properties rather than assessing the surface properties underneath the canopy (for a summary, see [2]).

Besides the effect of vegetation, the effect of moisture conditions will also play a role in determining the sensitivity of the radiometric signal to soil moisture. Soil emission decreases with increased moisture content, but a vegetation layer, such as a temperate deciduous or coniferous forest, will show the opposite effect and have a higher emission with increased water content [3], [4]. These opposite effects are due to the different physical behaviors of each layer in terms of absorption and scattering, and they complicate our understanding of the L-band signal above vegetated surfaces.

From the few previous experimental forest studies at L-band [5]–[8], a high accuracy of soil moisture retrieval over forests is not to be expected. Not only may the vegetation layer of tree canopy and understory be relatively dense, but in this type of environment, a litter layer is often an additional cover of the mineral soil. Studies over grasslands [9]–[11] have hinted at the fact that this layer could highly attenuate soil emission, although radiative transfer properties of litter are still largely unknown.

The Soil Moisture and Ocean Salinity (SMOS) mission of the European Space Agency will produce global measurements of soil moisture over land surfaces and salinity over the oceans on a temporal scale of two to three days [12], [13]. Pixel dimensions will be on the order of 40×40 km^2. It is easy to see that at this scale, many pixels will contain at least partial vegetation cover. In temperate, boreal, and tropical zones, forests are a major occurring vegetation type and will influence measurements in many pixels if not accounted for in the retrieval algorithms. However, *a priori* information on vegetation cover fraction will be available for SMOS, and if the emission behavior of forests is also known beforehand, it could be possible to retrieve accurate soil moisture values for the nonforested parts of the mixed pixel in some cases [14]. For this reason, the understanding of forest radiative transfer properties is an important aspect within the context of the SMOS.

The forward model used in the SMOS Level 2 Soil Moisture algorithm is the "L-band Microwave Emission of the Biosphere" (L-MEB) model [15]. This model is based on a

Manuscript received February 28, 2007; revised October 22, 2007.

J. P. Grant is with the Department of Hydrology and Geo-Environmental Sciences, Vrije Universiteit Amsterdam, 1081 HV Amsterdam, The Netherlands, and also with the Institut National de la Recherche Agronomique–Ecologie Fonctionnelle et Physique de l'Environnement, 33883 Bordeaux, France.

K. Saleh-Contell is with the Environmental Processes Group, Department of Geography, University of Cambridge, CB2 1TN Cambridge, U.K.

J.-P. Wigneron is with the Institut National de la Recherche Agronomique–Ecologie Fonctionnelle et Physique de l'Environnement, 33883 Bordeaux, France.

M. Guglielmetti was with the Institute of Terrestrial Ecosystems, Eidgenoessische Technische Hochschule (ETH) Zürich, 8092 Zürich, Switzerland.

Y. H. Kerr is with the Centre d'Etudes Spatiales de la Biosphère (CESBIO), 31401 Toulouse, France.

M. Schwank is with the Swiss Federal Institute for Forest, Snow and Landscape Research (WSL), 8903 Birmensdorf, Switzerland, and also with the Gamma Remote Sensing, 3073 Gümligen, Switzerland.

N. Skou is with the Danish National Space Center, Technical University of Denmark, 2800 Kongens Lyngby, Denmark.

A. A. Van de Griend, retired, was with the Department of Hydrology and Geo-Environmental Sciences, Vrije Universiteit Amsterdam, 1081 HV Amsterdam, The Netherlands.

Color versions of one or more of the figures in this paper are available online at http://ieeexplore.ieee.org

Digital Object Identifier 10.1109/TGRS.2007.914801

zero-order radiative transfer approach, which is often called the tau–omega (τ–ω) approach in the literature after the two vegetation parameters τ and ω, which are linked to canopy transmissivity and scattering, respectively. Although physically based, it is a relatively simple approach which is easy to use and does not require detailed information on the vegetation/soil layers beforehand, making it well suited to operational use at a global scale.

The inversion of L-MEB for the SMOS Level 2 Soil Moisture algorithm requires a calibration of the various soil and vegetation model parameters for different land cover types. Previous calibrations have included bare soils, grass, and various types of crops (for a summary, see [15]). This paper presents the first calibration of the forward model L-MEB over forests using experimental data. Previous forest studies in the context of SMOS were all based on modeling and/or very short-term experiments (e.g., [16] and [17]).

Parts of the coniferous and deciduous data sets used in this paper have previously been presented in [7] and [8], respectively. The main conclusions of those studies were the following: 1) branches are more important absorbers/emitters than leaves or trunks at L-band and 2) L-band variations in ground moisture over a medium dense forest (total aboveground biomass: $\sim$11 kg m^{-2}) with a distinctive litter layer are detectable, but they have too small a dynamic range to result in soil moisture retrieval with meaningful precision. Concerning litter, this paper does not focus specifically on that aspect, as the main purpose here was to calibrate the existing L-MEB algorithm over forests. Other studies are currently under progress to investigate the radiative transfer properties of such a layer.

This paper first gives an outline of the data sets and models used, including the description of a new experiment over conifers. Then, it presents the calibration of the relevant canopy and soil parameters in the L-MEB model, using experimental forest data. Results are given for two types of temperate forest (coniferous and deciduous), allowing for a general comparison. For the deciduous forest, a relationship between canopy optical depth and leaf area index (LAI) is also investigated. Finally, a sensitivity study is done for the focus parameters, temperature, soil moisture, and precipitation.

II. Materials

In this paper, three data sets were used. The first is the "Bray" data set, consisting of measurements over a coniferous forest stand. The second is the "FOSMEX" data set, consisting of measurements over a deciduous forest stand. The third data set consists of numerical simulations for three stands in Les Landes coniferous forest.

A. Bray Site and Data Set

The Bray site lies within the forest of Les Landes at approximately 20 km southwest of Bordeaux, France (latitude $44°42'$ N, longitude $0°46'$ W, and altitude 61 m) and consists of Maritime Pines (*Pinus pinaster* Ait). Tree age was 34 years at the time of measurement, resulting in a stand height of approximately 22 m. Maximum values for the canopy LAI are around 2.15, and the forest can thus be described as "medium dense." The understory consists mostly of grass (mainly *Molinia caerulea* L. Moench). Soils are sandy and hydromorphic podzols, with dark organic matter in the first 60 cm. On top of the soil lies a thick litter layer, the upper part of which consists mainly of dead grass, and the lower part consists of grass roots, pine needles, and other organic matter (humus).

Downward multiangular microwave measurements at Bray were made using the L-band (1.41 GHz) EMIRAD radiometer of the Technical University of Denmark [18]. These measurements were made from a 40-m-high tower at horizontal polarization and angles of 25°, 30°, 35°, 40°, 45°, 50°, 55°, and 60° from nadir. Full (-3 dB) antenna beamwidth was 25°, resulting in a $\sim$600 m^2 footprint at 45°. A thermal infrared scanner [Heitronics KT 15.85D (9.6–11.5 μm)] was fixed next to the radiometer to obtain measurements of surface temperature over the same area. Vertically polarized microwave measurements were found to be influenced by some kind of disturbance and were therefore not used. Simultaneous ground measurements were made of soil and litter temperature, soil and litter moisture content, and precipitation. The experiment was performed between July and December 2004 and is described in detail in [7].

Upward microwave measurements at Bray were made on February 22, 2006, again using the EMIRAD radiometer. The instrument was mounted on a structure [see Fig. 1 (top)], allowing it to take H- and V-polarized measurements of the forest at incidence angles between 90° and 0° relative to the upward vertical (zenith), as shown in Fig. 1 (middle). Three measurement series were taken at different azimuth angles, i.e., at 60°, 45°, and 0° (parallel) relative to the row direction of the trees [see Fig. 1 (bottom)]. Sky measurements were also taken for external calibration purposes, as explained in [7]. Sky brightness temperature calculated from [19] was $\sim$5 K.

B. Jülich Site and FOSMEX Data Set

The FOSMEX experiment took place at the Jülich site, which lies within a mixed deciduous forest in West Germany (latitude $6°\ 21'\ 30''$ E, longitude $50°\ 50'\ 30''$ N, and altitude 83 m). Within this site, the locations of the up- and downward radiometric measurements were in close proximity to each other. In the case of the upward measurements [8], the sole observed tree species was a 70-year-old Beech (*Fagus*) with an average crown height of approximately 20 m. At the location of the downward measurements [20], the forest comprised species of Oak (*Quercus*), Birch (*Betula*), and Beech (*Fagus*) in similar proportions. The tree age here was between 40 and 80 years old, and the average crown height was approximately 24 m. In general, the forest can be described as "rather dense." The ground surface is covered by a 0–5-cm-thick litter layer consisting of dead leaves, and the top 7 cm of the mineral soil also contains a large percentage of organic matter.

Downward radiometric measurements at Jülich were made during the whole of 2005, with two hiatuses between Julian Days 109–142 (April 19–May 22) and 227–280 (August 15–October 7). The ETH Zürich radiometers ELBARA (1.4 GHz; dual polarization [21]) and MORA (11.4 GHz; vertical polarization [22]) were installed on a 100-m-high tower over the forest. Multiangular measurements were taken at angles of 46°,

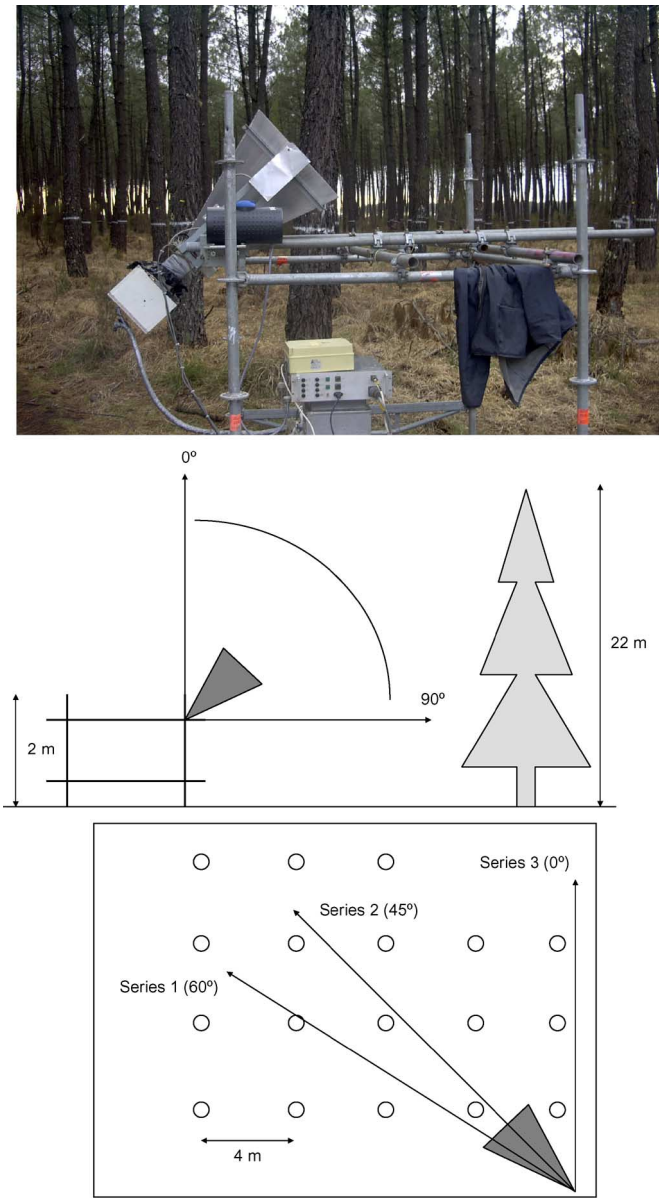

Fig. 1. (Top) Upward measurements of the canopy at the Bray site, using the EMIRAD L-band (1.4 GHz) radiometer mounted on a ∼2-m-high structure. (Middle) Schematic drawing (side view) of the experimental setup during the Bray upward measurements. Measurements were made at incidence angles between 0° and 90°, with 0° being the upward vertical. (Bottom) Schematic drawing of the Bray upward measurements, as shown from above. Trees are denoted by circles. Three series of measurements were made: at azimuth angles 60°, 45°, and 0° relative to the row direction of the trees.

50°, 54°, 58°, 62°, 66°, and 70° from nadir; however, only angles $< 60°$ were included in the final data set. Full (-3 dB) antenna beamwidth was 12°, resulting in a footprint of ~ 1200 m^2 at 46°. Simultaneous ground measurements of soil temperature and soil moisture content were taken, together with precipitation and air temperature at 20 m. This experiment is described in detail in [20].

Upward measurements at Jülich were made from September to November 2004 during the defoliation phase of the forest, again at multiple angles (40° and 60°) using the radiometers ELBARA and MORA. A detailed description of this experiment can be found in [8]. Soil surface temperatures were measured *in situ* with thermistors (Campbell S140 TL107) installed horizontally at 5 cm depth at 16 locations along two transects between the trees in order to give representative temperatures of the forest ground.

C. Synthetic Data Set Over Les Landes

Les Landes is a production forest in southwest France, consisting mainly of Maritime Pines (*Pinus pinaster* Ait). A synthetic brightness temperature data set was generated for the purposes of initialization and comparison with the Bray brightness temperature measurements described in Section II-A. The coniferous forest geometric database of [23] was used in combination with the Tor Vergata model (Section III-C) to produce simulated brightness temperatures, as also described in [24]. The synthetic data set includes the brightness temperatures of three populations of trees (5, 26, and 32 years old) at H and V polarizations, incidence angles 10°, 20°, 30°, 40°, and 50°, and soil moisture conditions from 0.05 to 0.4 m$^3 \cdot$ m^{-3} for a smooth soil of known temperature. The data set was compared with the "L-MEB" model (Section III-A) simulations, and optimum values of the necessary L-MEB parameters were retrieved.

III. Models

A. L-MEB

The L-MEB model [15] is based on a simplified (zero-order) radiative transfer equation, which is often called the tau–omega or τ–ω model in the literature [1], [25], [26]. In this model, multiple scattering is neglected, as is the reflection at the vegetation–atmosphere interface.

The main equation is as follows:

$$T_{\mathrm{B}}(\theta, P) = e_{\mathrm{s}} T_{\mathrm{s}} \gamma + (1-\omega)(1-\gamma) \times T_{\mathrm{c}} \left(1 + (1-e_{\mathrm{s}})\gamma\right) + T_{\mathrm{B,sky}}(1-e_{\mathrm{s}})\gamma^2. \quad (1)$$

The total brightness temperature T_{B} (dependent on the incidence angle θ and the polarization P) results from the addition of four terms: 1) the soil emission attenuated by the canopy layer; 2) the direct canopy emission; 3) the canopy emission reflected by the soil back through the canopy; and 4) the sky emission reflected by the soil and twice attenuated by the canopy layer. In this model, the subscripts "s" and "c" denote the "soil" and the "canopy," respectively. The sky brightness temperature $T_{\mathrm{B,sky}}$ was calculated according to [19]. The variable T is a thermodynamic temperature, e is the emissivity, and ω is the single scattering albedo of the canopy.

Finally, the variable γ describes the canopy transmissivity, which is related to the canopy optical depth τ according to

$$\gamma(\theta, P) = \exp(-\tau_0(\theta, P)/\cos\theta) \quad (2)$$

where $\tau_0(\theta, P)$ denotes the nadir (0°) optical depth calculated from an angular observation at angle θ. Dividing by the cosine corrects for the difference in physical length through the canopy layer at different angles, but it does not take into account the anisotropic effects of the canopy structure, which can change with the incidence angle depending on the orientation of the

canopy elements and the polarization of the measured signal. Therefore, the extra parameter $tt(P)$ has been introduced in the model to correct for the canopy structure

$$\tau_0(\theta, P) = \tau_{\mathrm{NAD}} \left(\sin^2(\theta) \cdot tt(P) + \cos^2(\theta)\right) \tag{3}$$

where the subscript "NAD" denotes the theoretical nadir values.

The soil emissivity e_{s} in (1) is calculated by

$$e_{\mathrm{s}}(\theta, P) = 1 - R_{\mathrm{s}}(\theta, P) \tag{4}$$

where R_{s} is the rough soil reflectivity. The Fresnel equations [3], [4] describe the reflectivity of a smooth soil (R^*_{s}) with a dielectric constant ε (calculated here using the method described in [27]); however, in reality, this rarely occurs. Therefore, a roughness correction is applied in the L-MEB model using a version of the semiempirical approach of [28]

$$R_{\mathrm{s}}(\theta, P) = R^*_{\mathrm{s}} \cdot \exp\Big(-H_{\mathrm{R}}(\theta, P) \cdot \cos^{N_{\mathrm{R}}(P)}(\theta)\Big). \tag{5}$$

H_{R} and N_{R} are the parameters describing the soil effective (physical and dielectrical) roughness and the angular dependence of this roughness, respectively.

When using this model, infrared temperatures were used for T_{c} and soil temperatures for T_{s} (1). In the case of the Bray site, the latter consisted of effective soil temperatures calculated over a depth of several times the wavelength λ, as described in [7]. For the Jülich site, profiles were not available, and measurements of soil temperature at 0–5 cm depth were used as input for T_{s}. As effective soil temperatures were found to lie close to soil temperatures at 2–3 cm depth at the Bray site [7], this is considered a valid approximation.

B. Upward Model

According to radiative transfer, when looking upward, the measured brightness temperatures (T_{B}) for incidence angles $< 90^\circ$ are composed of a vegetation and a sky component. As a first approximation, the soil emission reflected by the canopy is neglected. Equation (6) gives the model used for the analysis of the upward measurements of brightness temperature

$$T_{\mathrm{B}}(\theta, P) = (1 - \omega) \cdot (1 - \gamma) \cdot T_{\mathrm{c}} + T_{\mathrm{B,sky}} \cdot \gamma. \tag{6}$$

C. Tor Vergata Model

The Tor Vergata model [17], [29], [30] is based on the radiative transfer theory and uses a discrete approach, representing vegetation elements (trunks, branches, and leaves/needles) by geometrical shapes (cylinders) of suitable dimensions. The dielectric properties of each element are calculated using a semiempirical approach requiring information on moisture status [3].

Scattering and extinction cross sections of the crown and trunks are calculated according to the infinite length approximation. The understory layer is modeled as a simple absorbing layer, and the soil is represented by a uniform dielectric half-space with a rough interface. Soil permittivity is modeled using the semiempirical model of [27]. The soil bistatic scattering coefficient is obtained using the integral equation method [31].

By using the matrix doubling method [29], first, the scattering and extinction matrices of the whole crown are calculated, and then, the same algorithm is used to combine the crown with trunks, understory, and soil. In this way, the emissivity of the whole medium can be computed from the energy conservation law.

IV. Methods

A. Minimization

The inversion of L-MEB is done by minimizing a cost function CF [32]

$$\mathrm{CF} = \sum_{1}^{n} \frac{\left(T^{\circ}_{\mathrm{B}}(\theta, P) - T_{\mathrm{B}}(\theta, P)\right)^2}{\sigma^2_{T_{\mathrm{B}}}} + \sum_{1}^{n} \frac{\left(p_{\mathrm{i}} - p^{\mathrm{ini}}_{\mathrm{i}}\right)^2}{\sigma^2_{\mathrm{p}}}. \tag{7}$$

In the first term, the $^\circ$ symbol indicates the measured value of T_{B}. In the second term, p_{i} is the value of the retrieved parameter, and $p^{\mathrm{ini}}_{\mathrm{i}}$ is the initial value of each parameter in the retrieval process corresponding to an *a priori* estimate of the parameter p_{i}. σ^2 in the first term is the variance of the simulated values of T_{B}, and σ^2 in the second term is a fixed variance which can be used to constrain the model to a greater or lesser degree. The possibility of constraining parameters is built into the model for future processing of the SMOS observations, where a parameter can be constrained based on the previous day's value. However, in this paper, it was chosen to work without constraints (i.e., no *a priori* knowledge was assumed) in order to find the "real" optimum for each parameter. Therefore, the value $\sigma^2_{\mathrm{p}} = 1$ was used in all cases.

Parameter retrievals were assessed using the root mean-square error (RMSE) between the modeled and measured T_{B}. Several initializations for each parameter were tested in every case. For the Les Landes retrievals, no prior knowledge of possible initial values was available; therefore, the retrievals were additionally assessed using the efficiency of the regression or skill score (SS). Best fit canopy parameters were subsequently chosen by selecting initializations leading from $\min(\mathrm{RMSE})$ to $1.1 * (\min(\mathrm{RMSE}))$ and from $0.9 * (\max(\mathrm{SS}))$ to $\max(\mathrm{SS})$, and then taking the average of the resulting values.

B. Analysis Procedures

1) General: Before analyzing the data, all measurements for which rainfall occurred during the past 24 h were deleted from the data sets. Interception may lead to a significant increase in canopy opacity and a strong increase in the absorption and emission of the litter layer [11]. Under these types of conditions, it will become difficult to accurately retrieve the soil moisture. For this reason, an index which flags events during which interception effects are likely is built into the L-MEB model [15].

The six "focus parameters" throughout this paper were as follows: ω, τ_{NAD}, $tt(\mathrm{H})$, $tt(\mathrm{V})$, H_{R}, and N_{R}. In general, the approach taken was the following:

1) to retrieve the values of the canopy parameters ω, τ_{NAD}, $tt(\mathrm{H})$, and $tt(\mathrm{V})$ from the synthetic data set or the upward measurements;

2) to run the forward model (L-MEB) using the following in order to calculate the best fit values of the soil parameters H_{R} and N_{R}:
   a) the values found in step 1);
   b) the measured infrared and soil temperatures and soil moisture content;
   c) the downward radiometric measurements.

In step 1), simultaneous three- or four-parameter retrievals were done for each time of measurement using the upward model (6) together with (2) and (3) and the minimization method given by (7). In step 2), the best fit values of H_{R} were assumed to lie between 0 and 2, and those of N_{R} are between -2 and 2, as this is the range in which these values have generally been found in other studies [33]. Criteria for the best fit value here were the following: 1) lowest RMSE and 2) lowest bias, resulting between the observed and simulated values of T_{B}. The bias is a measure of the deviation of the observed-simulated values from the 1 : 1 line and was calculated as the average of $(T_{\mathrm{B,obs}} - T_{\mathrm{B,sim}})$ for all measurements.

2) Les Landes Synthetic Data (Coniferous): The canopy parameters ω, τ_{NAD}, $tt(\mathrm{H})$, and $tt(\mathrm{V})$ were simultaneously retrieved from the synthetic data set over Les Landes using the L-MEB model and the minimization method, as described in Section IV-A. In L-MEB, τ_{NAD} and ω are, in fact, effective and interdependent parameters, as the model is based on the assumption that scattering is predominantly in the forward direction [25]. For this reason, direct measurement of these parameters is not possible, and they can only be estimated from inverse modeling. Simultaneous retrieval of two interdependent parameters, such as τ_{NAD} and ω, will only give reliable results when no constraints are used during the retrieval and the data set is sufficiently large. For this last reason, a four-parameter retrieval was done only in the case of the synthetic data set. The value of ω found here for the 32-year-old population was then fixed during retrievals from the two experimental data sets (Bray and FOSMEX). The only known forest values for ω in the literature can be found in [34]; however, this procedure was applied over average conditions at a large scale, and it was therefore chosen to retrieve ω more specifically in this paper. Values found for the 32-year-old population for the other three vegetation parameters were used as initial values in the retrievals from the experimental data sets.

In addition to the aforementioned parameters, it was also possible to calculate the canopy structure parameter b from the synthetic data set. This parameter relates τ_{NAD} to the vegetation water content (VWC) by $\tau_{\mathrm{NAD}} = b^* \mathrm{VWC}$ [10] and was found to be related to different vegetation types by [35]. However, it does not take into account the effects of canopy anisotropy. Measurements over corn-covered [36] and grass-covered soils [37] have shown a rather pronounced dependence of transmissivity on polarization. To allow for such a possibility is the reason why (3) has been incorporated in the L-MEB model.

3) Bray Data (Coniferous): The upward measurements at Bray were used to simultaneously retrieve the values of τ_{NAD}, $tt(\mathrm{H})$, and $tt(\mathrm{V})$, again using the upward model and the minimization method described in Section IV-A. As explained in the previous paragraph (Section IV-B2), a fixed value of ω was taken from the Les Landes retrievals.

TABLE I
PARAMETER VALUES RESULTING FROM THE INVERSION OF THE L-MEB MODEL USING THE SYNTHETIC DATA SET OF LES LANDES. CALCULATIONS WERE DONE FOR CONIFEROUS FOREST STANDS OF THREE DIFFERENT AGES: 5, 26, AND 32 YEARS OLD. THE FIRST THREE ROWS GIVE THE PARAMETER VALUES USED IN THE DATA SIMULATION. THE FOLLOWING FIVE ROWS GIVE THE RETRIEVED L-MEB CANOPY PARAMETER VALUES TOGETHER WITH THE RESULTING RMSE IN EMISSIVITY, AND THE FINAL TWO ROWS SHOW THE b FACTOR CALCULATED FROM A COMBINATION OF THE ABOVE

	'5 years'	*'26 years'*	*'32 years'*
Tree density [trees/ha]	1421	497	368
Branch water content (BWC) [kg m^{-2}]	0.2	1.5	1.3
Total water content (TWC)[kg m^{-2}]	1	10	8
τ_{NAD}	0.30	0.60	0.66
tt(H)	0.41	0.59	0.62
tt(V)	0.18	0.36	0.47
ω	0.12	0.07	0.07
RMSE (emissivity) of retrievals	0.010	0.005	0.0035
b_{T} **tree structure parameter** ($\tau_0 = b_{\mathrm{T}} * \mathrm{TWC}$)	0.3	0.06	0.08
b_{Br} **branch structure parameter** ($\tau_0 = b_{\mathrm{Br}} * \mathrm{BWC}$)	1.5	0.4	0.51

It should be noted that some caution should be exercised with these results as the upward measurements at Bray were made with the radiometer placed at the edge of the forest. This could result in side-lobe effects leading to an underestimation of brightness temperature (from a higher sky influence), particularly at low angles (i.e., toward zenith). In addition, the side lobes could result in a relatively high influence of the ground surface at high angles, although this would be expected to result in a polarized signal, which was not apparent here. As a precaution, the beamwidth of the main lobe (Section II-A) plus the first side lobes (15° full beamwidth at half-power) was taken into consideration, and subsequently, only measurements between 30° and 60° were used.

4) FOSMEX Data (Deciduous): In the case of the FOSMEX data, the same procedure was used as described in the beginning of the previous paragraph (Section IV-B3) for the Bray data. In the upward model, T_{c} was set equal to the T_{air} measured at 20 m height. As the upward measurements were made continuously throughout three months, they resulted in a time series of each canopy parameter, which is something not available for the Bray site. During the upward measurements, defoliation was calculated through sampling of fallen leaf biomass (*LB*) (in $\mathrm{g} \cdot \mathrm{m}^{-2}$), as described in [8], and it was therefore possible to relate τ_{NAD} to LAI. The average value of $0.0172\ \mathrm{m}^2 \cdot \mathrm{g}^{-1}$ for the specific leaf area of Beech (*Fagus*) was taken from [38], as this was found to be irrespective of age and is an average value for sunlit and shady leaves [39]. Leaf water content measured at Jülich was around 50%. Thus, LAI was calculated as follows:

$$\mathrm{LAI} = 0.5 \cdot LB \cdot 0.0172 = 0.0086 \cdot LB. \tag{8}$$

V. RESULTS AND DISCUSSION

A. Les Landes Synthetic Data (Coniferous)

The results of parameter retrievals done over the synthetic data set of Les Landes are shown in Table I, together with the error associated with these retrievals (expressed by the RMSE in emissivity). The parameters for the 5- and 26-year-old populations are not validated in this paper but are included here as useful initial parameter values in the case of younger trees, as no

TABLE II
L-MEB PARAMETER VALUES FOUND FOR THE (CONIFEROUS) BRAY EXPERIMENT. (2a) RETRIEVED VALUES OF CANOPY PARAMETERS $\tau_{\rm NAD}$, $tt(\rm H)$, AND $tt(\rm V)$ FOR EACH OF THE THREE SERIES OF UPWARD MEASUREMENTS AT BRAY, TOGETHER WITH THE RESULTING VALUES OF RMSE. AVERAGE VALUES ± STANDARD DEVIATIONS ARE SHOWN FOR EACH PARAMETER. (2b) BEST FIT VALUES OF SOIL ROUGHNESS PARAMETERS H_R AND $N_R(\rm H)$ FOUND FOR THE BRAY DOWNWARD MEASUREMENTS, TOGETHER WITH THE RESULTING VALUES OF RMSE AND BIAS AFTER FORWARD MODELING WITH L-MEB

(2a)	τ_{NAD}	tt(H)	tt(V)	RMSE [K]
Series 1	0.66	0.83	0.81	1.5254
Series 2	0.64	1	0.92	1.9683
Series 3	0.71	0.83	0.67	2.3022
average ± stdev.	0.67 ± 0.04	0.89 ± 0.1	0.80 ± 0.13	

(2b)	H_R	$N_R(H)$	RMSE [K]	Bias [K]
H pol	1.2	1.8	3.7503	-0.0118

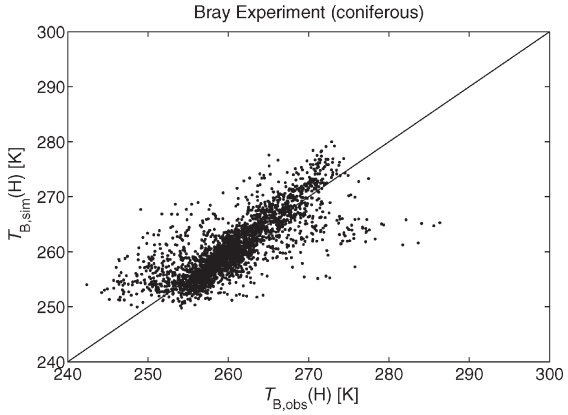

Fig. 2. Comparison of the observed ($T_{\rm B,obs}$) and the simulated ($T_{\rm B,sim}$) H-polarized brightness temperatures for the Bray experiment using the L-MEB forward model and downward measurements. Observations were excluded if rainfall had taken place during the past 24 h. Model parameter values were used as given in Table II. RMSE = 3.75 K; bias = −0.01 K.

other information is currently available. They also allow for a comparison between the emission of different populations, with the 26- and 32-year-old groups showing similar properties and the 5-year-old population dominated by higher transmissivity and scattering. The higher scattering could be due to a compensation effect of the model related to an underestimation of $\tau_{\rm NAD}$, as τ and ω are interrelated parameters (Section IV-B2). However, it could also be caused by the smaller distances between the scatterers in the case of young vegetation or by the different branch orientation in the 5-year-old population [23]. Further validation with experimental data will be necessary to fully understand this effect.

The value of ω found here for the 32-year-old population is similar to the values found in [34].

B. Bray Data (Coniferous)

Table II(a) shows the retrieved canopy parameter values of $\tau_{\rm NAD}$, $tt(\rm H)$, and $tt(\rm V)$ for each of the three series of upward measurements at the Bray site. As can be seen, the results of measurement series 1 and 2 are more similar, whereas series 3 is slightly different, probably as a result of the different azimuth angles relative to the row direction in this case (see Section II-A).

During the measurements made at the Bray site, the tree age was 34 years, and the retrieved canopy parameters can therefore be compared with those in the last column of Table I. The values of $\tau_{\rm NAD}$ are very similar in both cases; however, the $tt(P)$ parameters differ considerably. The upward measurements show a more isotropic canopy (i.e., $tt(P)$ closer to one) than that expected from the simulations. However, in both cases, $tt(\rm H) > tt(\rm V)$, indicating that the effect of anisotropy on transmissivity is stronger at the vertical polarization. The average values of $\tau_{\rm NAD}$, $tt(\rm H)$, and $tt(\rm V)$ shown in Table II(a) were used as input in the L-MEB model (3) to obtain the best fit values of the soil parameters H_R and $N_R(\rm H)$ from the downward Bray data. Resulting values of RMSE and bias between the measured and simulated values of $T_{\rm B}(\rm H)$ using the L-MEB model are shown in Table II(b). Fig. 2 shows a comparison of all observed and simulated H-polarized brightness temperatures.

C. FOSMEX Data (Deciduous)

Table III shows the resulting parameter values found for the FOSMEX data following the analysis procedure as described in Section IV-B4. Table III(a) shows the average ± standard deviation over time of the retrieved values of $\tau_{\rm NAD}$, $tt(\rm H)$, and $tt(\rm V)$.

The value for $\tau_{\rm NAD}$ in Table III(a) is the average over all defoliation states. In the case of a deciduous forest, a more realistic approach might be to relate $\tau_{\rm NAD}$ to the changing tree biomass throughout the year. However, by using the measurements made at Jülich, little to no correlation was found between $\tau_{\rm NAD}$ and LAI, as shown in Fig. 3. Using this type of relationship for LB monitoring over forests is therefore not recommended. However, this comes as no surprise, as other studies have previously shown [5], [8], [30] that at this frequency, branches, not leaves (or trunks), are the main sources of emission.

The average parameter values given in Table III(a) were used as input in the L-MEB model, after which the measured and simulated values of $T_{\rm B}$ were compared in order to find the best fit values of H_R, $N_R(\rm H)$, and $N_R(\rm V)$. These are shown together with the resulting values of RMSE and bias in Table III(b). Fig. 4 shows the result of forward modeling for all measurements at the H and V polarizations, respectively.

D. Comparison Between Experimental Data Sets

The results for both the Bray and the FOSMEX data lead to errors in brightness temperature (expressed by the RMSE and the bias) of a similar order of magnitude, although those for the Bray data set are slightly higher. However, some caution should be taken with a direct comparison of the RMSE values, as the two experiments were not exactly identical in terms of setup and measurements. Comparisons per parameter lead to the following conclusions. First, the canopy optical depth at nadir $\tau_{\rm NAD}$ is higher for the deciduous site, even when the LAI here is zero. Second, both sites show decreasing trends of $\tau_0(\theta, P)$ as a function of the incidence angle, i.e., $tt(\rm H)$ and $tt(\rm V)$ are both <1. In the case of an isotropic canopy, $tt(P) = 1$. The fact that

TABLE III
L-MEB PARAMETER VALUES FOUND FOR THE (DECIDUOUS) FOSMEX EXPERIMENT. (3a) UP = UPWARD DATA SET. AVERAGE VALUES ± STANDARD DEVIATIONS OVER TIME OF THE RETRIEVED VALUES OF CANOPY PARAMETERS τ_{NAD}, $tt(\mathrm{H})$, AND $tt(\mathrm{V})$, TOGETHER WITH THE RESULTING VALUES OF RMSE. (3b) DOWN = DOWNWARD DATA SET. BEST FIT VALUES OF SOIL ROUGHNESS PARAMETERS H_R, $N_R(\mathrm{H})$, AND $N_{\mathrm{R}}(\mathrm{V})$, TOGETHER WITH THE RESULTING VALUES OF RMSE AND BIAS FOR BOTH POLARIZATIONS AFTER FORWARD MODELING WITH L-MEB

(3a)	τ_{NAD}	$tt(H)$	$tt(V)$	RMSE [K]
UP	0.98 ± 0.08	0.54 ± 0.09	0.43 ± 0.06	1.7239 ± 0.7859

(3b)				H pol		V pol	
	H_R	$N_R(H)$	$N_R(V)$	RMSE [K]	Bias [K]	RMSE [K]	Bias [K]
DOWN	1	1	2	2.791	-0.009	3.194	0.680

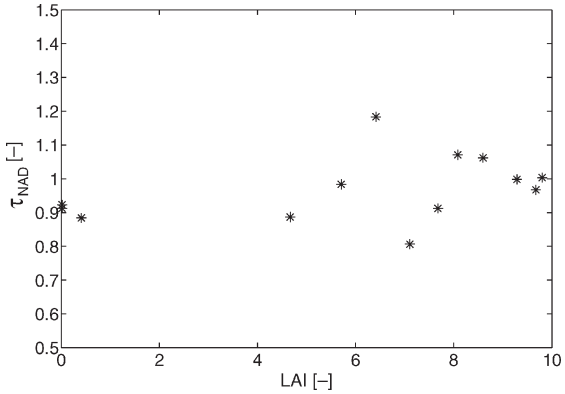

Fig. 3. LAI [from (8)] plotted against the retrieved values of τ_{NAD} during the defoliation period at the Jülich site (FOSMEX data set).

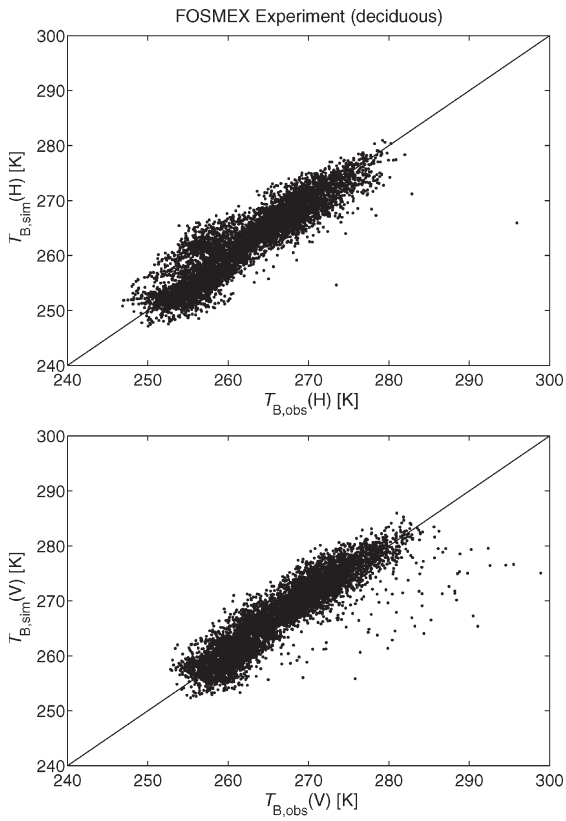

Fig. 4. Comparison of the observed ($T_{\mathrm{B,obs}}$) and the simulated ($T_{\mathrm{B,sim}}$) (top) H- and (bottom) V-polarized brightness temperatures for the FOSMEX experiment using the L-MEB forward model and downward measurements. Observations were excluded if rainfall had taken place during the past 24 h. Model parameter values were used as given in Table III. H-pol: RMSE = 2.79 K; bias = −0.01 K. V-pol: RMSE = 3.19 K; bias = 0.68 K.

the angular dependence is more pronounced over the deciduous site (i.e., lower values of $tt(P)$ are found; see Tables II and III) therefore indicates that this canopy is less isotropic than that at the coniferous site. Third, the ratios between $tt(\mathrm{V})$ and $tt(\mathrm{H})$ (called rtt in L-MEB) are 0.90 and 0.80 for the Bray and FOSMEX data sets, respectively, showing that, at both sites, the effect of anisotropy on canopy transmissivity and emissivity is greater at the vertical polarization. From (2) and (3), it follows that when $tt(\mathrm{V})$ is lower than $tt(\mathrm{H})$, transmissivity will be higher at V polarization and canopy emissivity $(1-\omega)(1-\gamma)$ will therefore be lower. This confirms that at L-band, the influence of vertically oriented canopy elements, such as trunks, is limited, and horizontal elements, such as branches, play a greater role as a source of scattering and absorption, as noted in the previous paragraph (Section V-C). Finally, concerning the soil roughness parameters H_R and N_R, it can be concluded that there is no significant difference in roughness between the two forests, both resulting in a best fit when $H_R \approx 1$, which corresponds to a rather high surface emission (5). The angular dependence of the roughness at the horizontal polarization, as expressed by $N_R(\mathrm{H})$, is lower for the FOSMEX data than for the Bray data, which is possibly due to the difference in litter-layer thickness between both sites. As expected, the understory/litter layer at Jülich is thinner than that at Bray because although the deciduous tree species generally produce more litter, decomposition is generally also faster than in the case of the coniferous forests [40], [41]. A thicker litter layer can be expected to attenuate more of the soil signal and consequently have a higher self-emission. However, the various aspects governing the behavior of the H_R and N_R parameters are still relatively unknown, and here, they can mainly be seen as (effective) fitting parameters although, in other studies, the H_R parameter was found to be a function of soil moisture in the cases of bare soil and grass covers ([33] and [42], respectively). Future research will have to show whether this is also the case under forests; however, in this paper, no such relationship was found.

E. Sensitivity Study

A sensitivity study was conducted by using the calibrated parameter values (from Tables II and III) in the L-MEB model

TABLE IV
VALUES OF RMSE AND BIAS IN T_B FOUND AFTER FORWARD MODELING WITH L-MEB WHEN VARIOUS TYPES OF ERRORS ARE INCLUDED IN THE DATA, RESPECTIVELY: (a) ERRORS IN L-MEB CANOPY AND SOIL ROUGHNESS PARAMETERS. (b) ERRORS IN TEMPERATURE AND SOIL MOISTURE. (c) INCLUDING MEASUREMENTS WHERE PRECIPITATION HAS TAKEN PLACE DURING THE PAST 24 h. RESULTS (IN [K]) ARE SHOWN FOR BOTH BRAY AND FOSMEX (DOWNWARD) DATA SETS

(4a)		***Bray (H)***	***FOSMEX (V)***	***FOSMEX (H)***
(0) reference	RMSE	3.7503	3.194	2.791
	Bias	-0.0118	0.680	-0.009
(1) *tt*(H) = *tt*(V) = 1	RMSE	3.9688	3.1730	4.1465
	Bias	0.7905	0.6039	2.7638
(2) ω = 0	RMSE	13.7688	14.4618	15.0988
	Bias	13.0381	14.0762	14.7977
(3) H_R = 0	RMSE	14.6763	3.9350	8.0307
	Bias	-13.1282	-1.4293	-7.4224
(4) N_R = +1 (H), -1 (V)	RMSE	4.0182	3.4248	2.7910
	Bias	0.5057	1.5698	-0.0093

(4b)		***Bray (H)***	***FOSMEX (V)***	***FOSMEX (H)***
(5) +2 K	RMSE	4.1747	4.0533	3.3491
	Bias	1.8351	2.5835	1.8511
(6) +0.04 m^3m^{-3}	RMSE	3.8262	3.1445	2.8554
	Bias	-0.6704	-0.0441	-0.5374

(4c)		***Bray (H)***	***FOSMEX (V)***	***FOSMEX (H)***
(7a) + rain, all data	RMSE	3.8317	3.2013	2.7398
	Bias	0.4067	0.2465	-0.6388
(7b) + rain, leaves	RMSE	-	3.3318	2.4265
	Bias	-	0.7832	-0.6650
(7c) + rain, no leaves	RMSE	-	3.0786	2.9967
	Bias	-	-0.2404	-0.6144

as a reference situation, then introducing an error in one particular variable, and running the forward model. The study consists of three parts: 1) errors introduced in the canopy and soil roughness parameters; 2) errors introduced in the physical temperatures and soil moisture values; and 3) including observations where precipitation had taken place during the previous 24 h. Table IV(a)–(c) shows the respective results in terms of RMSE and bias in T_B.

First shown in Table IV(a) are the reference values, as found in Sections V-B and C (Tables II and III). When the assumption of an isotropic canopy is made in case (1), i.e., $tt(\mathrm{H})$ and $tt(\mathrm{V})$ are set to one, the errors increase for the H polarization, slightly with the Bray data but more so with the FOSMEX data set, resulting in model overestimations of $\sim$1–3 K in $T_B(\mathrm{H})$, respectively. At V polarization, there is hardly any change in errors. As the main part of canopy emission is determined by horizontally oriented elements (e.g., branches), T_B at H polarization will be more affected by a possibly erroneous assumption of isotropy. Second, the assumption of no scattering, i.e., $\omega = 0$, was tested in case (2). This led to very high errors in both the RMSE and the bias. The parameters ω and τ are interdependent, as mentioned previously (Section IV-B2), and the values of τ_{NAD} in this paper are based on the situation where $\omega = 0.07$. High errors are therefore not surprising; however, this does illustrate how sensitive the L-MEB model is to the erroneous values of ω for a given value of τ_{NAD}.

In case (3), the assumption of a smooth soil was tested by setting H_R to zero, which led to a high error with the Bray data. The errors with the FOSMEX data set were smaller, but it is interesting to see that at H polarization, they are more than double those at V polarization. This is opposite to the results predicted by the physically based air-to-soil transition model in [4]. However, the latter evaluation assumed isotropic soil permittivities, and in doing so, it did not consider for any prevailing orientation of structures in the surface layer. The conflicting results found in this paper indicate that the assumption made on the isotropic soil permittivity might not be correct in the case of litter-covered soils or soils with a high percentage of organic matter.

In [33], it is found that for a bare loamy soil, the best fit values of N_R were $+1$ at H polarization (which is close to the values found in this paper) and -1 at V polarization. Using these values in case (4) led to greater errors at H polarization with the Bray data and at V polarization with the FOSMEX data, as expected from the fact that the values found in these two cases for $N_R(P)$ (see Tables II and III) differed most from ± 1. However, these errors are much smaller than those found for erroneous values of H_R, and we can conclude that H_R has a much greater influence on modeling of the ground layer (soil and litter).

In Table IV(b), case (5) shows the results when a constant $+2$ K error is added to both the soil and canopy temperatures, and case (6) has a constant $+0.04$ $\mathrm{m}^3 \cdot \mathrm{m}^{-3}$ error added to

the measured values of the soil moisture. The value of 0.04 $m^3 \cdot m^{-3}$ was chosen bearing in mind that this is the SMOS anticipated accuracy for the soil moisture retrievals. The 2 K error in temperature is often used in this type of modeling study. Cases (5) and (6) show expected behavior: Case (5) shows that a 2 K increase in temperature leads to an $\sim$2 K model overestimation (expected from the relationship $T_{\rm B} \approx T * e$), and in case (6), an increase in soil moisture, of course, leads to a (small) model underestimation, as the soil emissivity reduces with an increasing moisture content. As expected, the resulting differences in RMSE compared with the reference situation are very small, in line with the knowledge that sensitivity to soil moisture is very low over forested areas.

Table IV(c) shows the effect of including rainfall data (observations where precipitation took place during the previous 24 h) in the forward model. During the Bray experiment, precipitation occurred 8.2% of the time versus 9.6% of the time during FOSMEX. Minimum, maximum, and average precipitation values of all rainfall periods at Bray were 0.2, 17.8, and 1.2 mm/h, respectively. At the Jülich site, the respective values were 0.1, 16.7, and 0.8 mm/h. As mentioned previously (Section IV-B1), canopy emission may increase significantly during rainfall. However, in this paper, the inclusion of rainfall data only led to very small differences in errors in all cases: a slight overestimation with the Bray data and a slight underestimation with the FOSMEX data (case 7a). Because a large part of intercepted precipitation is caught by leaves (needles), the FOSMEX data were additionally split into a subset with leaves (April 17–November 23) and without (remaining days) to investigate whether this would lead to a significant difference in error. However, as the results show (cases 7b and 7c, respectively), the differences in RMSE and bias found here are small in all cases, although the effects at the H and V polarizations are reversed. At the V polarization, the error increases for the "leaves" situation, whereas at the H polarization, this happens for the "no leaves" situation.

VI. Summary and Conclusion

By using up- and downward L-band measurements over a coniferous and a deciduous forest together with a synthetic L-band data set over conifers, a calibration was made of the L-MEB model used in the SMOS Level 2 Soil Moisture algorithm. This has resulted in working values of the main canopy and soil roughness parameters $\tau_{\rm NAD}$, ω, $tt({\rm H})$, $tt({\rm V})$, H_R, and N_R, as shown in Tables I–III. Using these values in the forward model resulted in an RMSE in brightness temperatures from 2.8 to 3.8 K, depending on the data set and polarization.

Previously, the "$\tau-\omega$"-type modeling approaches at L-band are often corrected for the dependence of canopy optical depth on incidence angle by dividing by the cosine of the angle. However, this corrects for the difference in path length only, and not for the difference in structure (i.e., polarization effects), encountered at different angles. The canopy optical depth was still found to decrease with increasing incidence angle for both forest types after a "cosine" correction. At both sites, this effect on optical depth was stronger for the V polarization than for the H polarization. This paper therefore shows that an additional angular correction using the $tt(P)$ parameter in the L-MEB model is essential for nonisotropic canopies.

At L-band, leaves are not the main sources of emission, and little to no correlation was found between the canopy optical depth and the LAI for the deciduous site. Using this type of relationship for LB monitoring over forests is therefore not recommended at this wavelength.

A sensitivity study was conducted by introducing various types of errors in the L-MEB parameter values, then running the forward model, and assessing the effect on $T_{\rm B}(P)$ in terms of RMSE and bias. In most cases, the errors were small. Even when the observations where precipitation had taken place during the previous 24 h were included in the analysis, this resulted in only a very slight increase in RMSE. However, the model was found to be very sensitive to the erroneous values of ω for a given value of $\tau_{\rm NAD}$, which is most likely because these two parameters are interdependent.

The results found in this paper will be integrated in the operational SMOS Level 2 algorithm and used in future inversions of the L-MEB for soil moisture retrievals over heterogeneous, partly forested areas.

Acknowledgment

The authors would like to thank A. Kruszewski of INRA, Bordeaux, for his skilled help with the Bray upward measurements and the Department of Computer Science, Systems and Production of Tor Vergata University for generating the simulated brightness temperatures with the Tor Vergata model resulting in the synthetic data set. The Jülich downward experiment (FOSMEX) was supported in part by the German Research Foundation funded project: "Combining remote sensing and geophysical methods for monitoring and modeling of water fluxes and soil water dynamics in a forest stand."

References

[1] K. P. Kirdyashev, A. A. Chukhlantsev, and A. M. Shutko, "Microwave radiation of the earth's surface in the presence of vegetation cover," *Radiotekhnika*, vol. 24, pp. 256–264, 1979.

[2] P. Pampaloni, "Microwave radiometry of forests," *Waves Random Media*, vol. 14, no. 2, pp. S275–S298, Apr. 2004.

[3] F. Ulaby, R. Moore, and A. Fung, *Microwave Remote Sensing: Active and Passive*, vol. III. Dedham, MA: Artech House, 1986.

[4] C. Mätzler, Ed., *Thermal Microwave Radiation—Applications for Remote Sensing*, IET Electromagnetic Waves Series No. 52, London, U.K.: IET, 2006.

[5] G. Macelloni, S. Paloscia, P. Pampaloni, and R. Ruisi, "Airborne multifrequency L- to Ka-band radiometric measurements over forests," *IEEE Trans. Geosci. Remote Sens.*, vol. 39, no. 11, pp. 2507–2513, Nov. 2001.

[6] R. H. Lang, C. Utku, P. de Matthaeis, N. Chauhan, and D. M. Le Vine, "ESTAR and model brightness temperatures over forests: Effects of soil moisture," in *Proc. IGARSS*, 2001, vol. 3, pp. 1300–1302.

[7] J. P. Grant, J.-P. Wigneron, A. A. Van de Griend, A. Kruszewski, S. Schmidl Søbjærg, and N. Skou, "A field experiment on microwave forest radiometry: L-band signal behaviour for varying conditions of surface wetness," *Remote Sens. Environ.*, vol. 109, no. 1, pp. 10–19, Jul. 2007.

[8] M. Guglielmetti, M. Schwank, C. Mätzler, C. Oberdörster, J. Vanderborght, and H. Flühler, "Measured microwave radiative transfer properties of a deciduous forest canopy," *Remote Sens. Environ.*, vol. 109, no. 4, pp. 523–532, Aug. 2007.

[9] T. J. Schmugge, J. R. Wang, and G. Asrar, "Results from the push broom microwave radiometer flights over the Konza Prairie in 1985," *IEEE Trans. Geosci. Remote Sens.*, vol. 26, no. 5, pp. 590–596, Sep. 1988.

[10] T. J. Jackson and T. J. Schmugge, "Vegetation effects on the microwave emission of soils," *Remote Sens. Environ.*, vol. 36, no. 3, pp. 203–212, Jun. 1991.

[11] K. Saleh, J.-P. Wigneron, P. de Rosnay, J.-C. Calvet, M.-J. Escorihuela, Y. H. Kerr, and P. Waldteufel, "Impact of rain interception by vegetation and mulch on the L-band emission of natural grass," (SMOSREX experiment), *Remote Sens. Environ.*, vol. 101, no. 1, pp. 127–139, Mar. 2006.
[12] Y. H. Kerr, P. Waldteufel, J.-P. Wigneron, J.-M. Martinuzzi, J. Font, and M. Berger, "Soil moisture retrieval from space: The Soil Moisture and Ocean Salinity (SMOS) mission," *IEEE Trans. Geosci. Remote Sens.*, vol. 39, no. 8, pp. 1729–1735, Aug. 2001.
[13] M. Berger, Y. H. Kerr, J. Font, J.-P. Wigneron, J.-C. Calvet, K. Saleh, E. Lopez-Baeza, L. Simmonds, P. Ferrazzoli, B. Van de Hurk, P. Waldteufel, F. Petitcolin, A. A. Van de Griend, E. Attema, and M. Rast, "Measuring the moisture in the earth's soil—Advancing the science with ESA's SMOS mission," *ESA Bull.*, vol. 115, pp. 40–45, 2003.
[14] A. A. Van de Griend, J.-P. Wigneron, and P. Waldteufel, "Soil moisture retrieval from heterogeneous surfaces by 1.4 GHz multi-angle SMOS observations using 'a priori knowledge' of surface cover fractions," in *Proc. IGARSS*, 2004, vol. 7, pp. 4552–4555.
[15] J.-P. Wigneron, Y. H. Kerr, P. Waldteufel, K. Saleh, M.-J. Escorihuela, P. Richaume, P. Ferrazzoli, P. de Rosnay, R. Gurney, J.-C. Calvet, J. P. Grant, M. Guglielmetti, B. Hornbuckle, C. Mätzler, T. Pellarin, and M. Schwank, "L-band microwave emission of the biosphere (L-MEB) model: Description and calibration against experimental data sets over crop fields," *Remote Sens. Environ.*, vol. 107, no. 4, pp. 639–655, Apr. 2007.
[16] K. Saleh, J.-P. Wigneron, J.-C. Calvet, E. Lopez-Baeza, P. Ferrazzoli, M. Berger, P. Wursteisen, L. Simmonds, and J. Miller, "The EuroSTARRS airborne campaign in support of the SMOS mission: First results over land surfaces," *Int. J. Remote Sens.*, vol. 25, no. 1, pp. 177–194, Jan. 2004.
[17] A. Della Vecchia, K. Saleh, P. Ferrazzoli, L. Guerriero, and J.-P. Wigneron, "Simulating L-band emission of coniferous forests using a discrete model and a detailed geometrical representation," *IEEE Geosci. Remote Sens. Lett.*, vol. 3, no. 3, pp. 364–368, Jul. 2006.
[18] S. Schmidl Søbjærg, "Polarimetric radiometers and their applications," Ph.D. dissertation, Tech. Univ. Denmark, Lyngby, Denmark, 2002.
[19] T. Pellarin, J.-P. Wigneron, J.-C. Calvet, M. Berger, H. Douville, P. Ferrazzoli, Y. H. Kerr, E. Lopez-Baeza, J. Pulliainen, L. Simmonds, and P. Waldteufel, "Two-year global simulation of L-band brightness temperatures over land," *IEEE Trans. Geosci. Remote Sens.*, vol. 41, no. 9, pp. 2135–2139, Sep. 2003.
[20] M. Guglielmetti, M. Schwank, C. Mätzler, C. Oberdörster, J. Vanderborght, and H. Flühler, "FOSMEX: Forest soil moisture experiments with microwave radiometry," *IEEE Trans. Geosci. Remote Sens.*, vol. 46, no. 3, pp. 727–735, Mar. 2008.
[21] C. Mätzler, D. Weber, M. Wüthrich, K. Schneeberger, C. Stamm, and H. Flühler, "ELBARA, the ETH L-band radiometer for soil moisture research," in *Proc. IGARSS*, 2003, vol. 5, pp. 3058–3060.
[22] Institute for Applied Physics, *Handbook of the MORA 11.4 GHz Radiometer*, 1991, Bern, Switzerland: Univ. Bern.
[23] K. Saleh, A. Porté, D. Guyon, P. Ferrazzoli, and J.-P. Wigneron, "A forest geometric description of a Maritime pine forest suitable for discrete microwave models," *IEEE Trans. Geosci. Remote Sens.*, vol. 43, no. 9, pp. 2024–2035, Sep. 2005.
[24] K. Saleh, L. Guerriero, A. Della Vecchia, P. Ferrazzoli, J.-P. Wigneron, A. Porté, D. Guyon, and I. Champion, "A radiative model to simulate forest emission at L-band: Sensitivity of brightness temperature to forest components," in *Proc. IGARSS*, 2004, vol. 2, pp. 1025–1028.
[25] T. Mo, B. J. Choudhury, T. J. Schmugge, J. R. Wang, and T. J. Jackson, "A model for microwave emission from vegetation-covered fields," *J. Geophys. Res.*, vol. 87, no. C13, pp. 11 229–11 237, 1982.
[26] J.-P. Wigneron, A. Chanzy, J.-C. Calvet, and N. Bruguier, "A simple algorithm to retrieve soil moisture and vegetation biomass using passive microwave measurements over crop fields," *Remote Sens. Environ.*, vol. 51, no. 3, pp. 331–341, Mar. 1995.
[27] M. C. Dobson, F. T. Ulaby, M. T. Hallikainen, and M. A. El-Rayes, "Microwave dielectric behavior of wet soil—Part II: Dielectric mixing models," *IEEE Trans. Geosci. Remote Sens.*, vol. GRS-23, no. 1, pp. 35–46, Jan. 1985.
[28] J. R. Wang and B. J. Choudhury, "Remote sensing of soil moisture content over bare field at 1.4 GHz frequency," *J. Geophys. Res.*, vol. 86, no. C6, pp. 5277–5282, 1981.
[29] P. Ferrazzoli and L. Guerriero, "Passive microwave remote sensing of forests: A model investigation," *IEEE Trans. Geosci. Remote Sens.*, vol. 34, no. 2, pp. 433–443, Mar. 1996.
[30] P. Ferrazzoli, L. Guerriero, and J.-P. Wigneron, "Simulating L-band emission of forests in view of future satellite applications," *IEEE Trans. Geosci. Remote Sens.*, vol. 40, no. 12, pp. 2700–2708, Dec. 2002.
[31] A. K. Fung, *Microwave Scattering and Emission Models and Their Applications*. Norwood, MA: Artech House, 1994.
[32] M. Pardé, J.-P. Wigneron, A. Chanzy, Y. H. Kerr, J.-C. Calvet, P. Waldteufel, S. Schmidl Søbjærg, and N. Skou, "N-parameter retrievals from L-band microwave observations acquired over a variety of crop fields," *IEEE Trans. Geosci. Remote Sens.*, vol. 42, no. 6, pp. 1168–1178, Jun. 2004.
[33] M.-J. Escorihuela, Y. H. Kerr, P. de Rosnay, J.-P. Wigneron, J.-C. Calvet, and F. Lemaître, "A simple model of the bare soil microwave emission at L-band," *IEEE Trans. Geosci. Remote Sens.*, vol. 45, no. 7, pp. 1978–1987, Jul. 2007.
[34] A. Della Vecchia, P. Ferrazzoli, F. Giorgio, L. Guerriero, "A large scale approach to estimate L band emission from forest covered surfaces," in *Proc. 2nd Recent Adv. Quantitative Remote Sens.*, J. A. Sobrino, Ed., Valencia, Spain, 2006, pp. 925–930.
[35] A. A. Van de Griend and J.-P. Wigneron, "The b-factor as a function of frequency and canopy type at H-polarization," *IEEE Trans. Geosci. Remote Sens.*, vol. 42, no. 4, pp. 786–794, Apr. 2004.
[36] B. K. Hornbuckle, A. W. England, R. D. De Roo, M. A. Fischman, and D. L. Boprie, "Vegetation canopy anisotropy at 1.4 GHz," *IEEE Trans. Geosci. Remote Sens.*, vol. 41, no. 10, pp. 2211–2223, Oct. 2003.
[37] M. Schwank, C. Mätzler, M. Guglielmetti, and H. Flühler, "L-band radiometer measurements of soil water under growing clover grass," *IEEE Trans. Geosci. Remote Sens.*, vol. 43, no. 10, pp. 2225–2237, Oct. 2005.
[38] H. H. Bartelink, "Allometric relationships for biomass and leaf area of Beech (*Fagus sylvatica* L.)," *Ann. Sci. For.*, vol. 54, no. 1, pp. 39–50, 1997.
[39] E. Masarovicova, A. Cicak, and I. Stefancik, "Ecophysiological, biochemical, anatomical and productional characteristics of Beech (*Fagus sylvatica* L.) leaves from regions with different degree of immission impact," *Ecologia*, vol. 15, no. 3, pp. 337–351, 1996. (Bratislava).
[40] V. A. Kavvadias, D. Alifragis, A. Tsiontsis, G. Brofas, and G. Stamatelos, "Litterfall, litter accumulation and litter decomposition rates in four forest ecosystems in northern Greece," *For. Ecol. Manage.*, vol. 144, no. 1–3, pp. 113–127, Apr. 2001.
[41] T. Osono and H. Takeda, "Fungal decomposition of *Abies* needle and *Betula* leaf litter," *Mycologia*, vol. 98, no. 2, pp. 172–179, Mar. 2006.
[42] K. Saleh, J.-P. Wigneron, P. Waldteufel, P. de Rosnay, M. Schwank, J.-C. Calvet, and Y. H. Kerr, "Estimates of surface soil moisture under grass covers using L-band radiometry," *Remote Sens. Environ.*, vol. 109, no. 1, pp. 42–53, Jul. 2007.

Jennifer P. Grant received the M.S. degree in environmental sciences from Vrije Universiteit (VU) Amsterdam, Amsterdam, The Netherlands, in 2001, where she is currently working toward the Ph.D. degree in the Department of Hydrology and Geo-Environmental Sciences in collaboration with the Institut National de la Recherche Agronomique–Ecologie Fonctionnelle et Physique de l'Environnement, Bordeaux, France.

Her research focuses on the measurement and modeling of L-band passive microwave emission of forests for future soil moisture retrieval from SMOS observations.

Kauzar Saleh-Contell received the B.S. degree in physics and the Ph.D. degree in 2006 from the University of Valencia, Valencia, Spain.

She was with the Institut National de la Recherche Agronomique, Bordeaux, France, during her Ph.D., and she is currently with the Environmental Processes Group, Department of Geography, University of Cambridge, Cambridge, U.K. Her research focuses on the retrieval of soil and vegetation properties from L-band passive microwaves, particularly in prairies and forests. Current activities include tests of the European Space Agency SMOS mission soil moisture retrieval algorithm from airborne measurements at L-band.

Jean-Pierre Wigneron (M'97–SM'03) received the Engineering degree from SupAéro, Ecole Nationale Supérieure de l'Aéronautique et de l'Espace (ENSAE), Toulouse, France, in 1987 and the Ph.D. degree from the University of Toulouse, Toulouse, in 1993.

He is currently a Senior Research Scientist with the Institut National de Recherche Agronomique (INRA), Bordeaux, France, where he is also the Head of the remote sensing group, Ecologie Fonctionnelle et Physique de l'Environnement (EPHYSE). He coordinated the development of the L-MEB model for soil and vegetation in the level-2 inversion algorithm of the ESA's SMOS Mission. He was a Principal Investigator of several international campaigns in the field of microwave remote sensing. His research interests include microwave remote sensing of soil and vegetation, radiative transfer, and data assimilation. Since 2005, he has been a Member of the editorial board of *Remote Sensing of Environment*.

Massimo Guglielmetti studied environmental sciences at the Eidgenoessische Technische Hochschule (ETH), Zürich, Switzerland. The topic of his master thesis in soil physics in 2003 was "Quantitative description of tracer distribution in heterogenic sands." He received the Ph.D. degree in environmental sciences from ETH in 2007. The topic of his Ph.D. was inferring forest soil water content with microwave radiometry.

Yann H. Kerr (M'88–SM'01) received the Engineering degree from the École Nationale de la Statistique et de l'Administration Économique, Malakoff Cedex, France, the M.Sc. degree in electronics and electrical enginering from Glasgow University, Glasgow, U.K., and the Ph.D. degree from Université Paul Sabatier, Toulouse, France.

From 1980 to 1985, he was with the Centre National d'Études Spatiales. In 1985, he was with the Laboratoire d'Etudes et de Recherches Télédétection Spatiale. He spent 19 months with the Jet Propulsion Laboratory, Pasadena, CA, from 1987 to 1988. Since 1995, he has been working with the Centre d'Etudes Spatiales de la Biosphère (CESBIO), Toulouse. His fields of interest include the theory and techniques for microwave and thermal infrared remote sensing of the Earth, with emphasis on hydrology, water resources management, and vegetation monitoring. He was an EOS Principal Investigator (interdisciplinary investigations). He was the Science Lead on the MIRAS project for the European Space Agency and is currently the Lead Investigator of the Soil Moisture and Ocean Salinity mission.

Mike Schwank received the Ph.D. degree in physics from the Swiss Federal Institute of Technology, Zürich, Switzerland, in 1999. The topic of his Ph.D. was "Nanolithography using a high-pressure scanning-tunneling microscope."

In the following three years, he gained experience in the industrial environment, where he worked as a Research and Development Engineer in the field of micro-optics. Since 2003, he has been working in the research field of microwave remote sensing applied to soil moisture detection. Currently, he works as a Senior Research Assistant with the Swiss Federal Institute for Forest, Snow and Landscape Research (WSL), Birmensdorf, Switzerland. His research involves practical and theoretical aspects of microwave radiometry. In addition to his research, he also works for the company Gamma Remote Sensing, Gümligen, Switzerland, where he is involved in the production of microwave radiometers to be deployed for ground-based SMOS calibration/validation purposes.

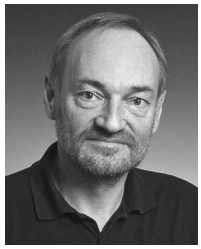

Niels Skou (S'78–M'79–SM'96–F'03) received the M.Sc., Ph.D., and D.Sc. degrees from the Technical University of Denmark (DTU), Lyngby, in 1972, 1981, and 1990, respectively.

He is currently a Professor with the Danish National Space Center, DTU. His research has been directed toward microwave remote sensing systems. After working for three years on the development of radar systems for measuring ice sheets in Greenland and Antarctica, his interest turned toward microwave radiometry. He developed a scanning multifrequency airborne radiometer system. After that, his subjects were radiometer measurements of sea ice and oil pollution on the sea, spaceborne radiometer systems, and development of new systems for specific purposes. In the mid-1980s, his interest turned back to active instruments, and he became engaged in the development of an airborne, multifrequency, polarimetric, and interferometric synthetic aperture radar system—with special emphasis on calibration fidelity. However, his activities within microwave radiometry have continued, mainly within the areas of synthetic aperture radiometry and polarimetric radiometry. The work on synthetic aperture radiometry has led to the SMOS mission, which is one of the European Space Agency's Earth Explorer Opportunity Missions, and he is currently heavily involved in this project, for example, as a member of the SMOS Science Advisory Group.

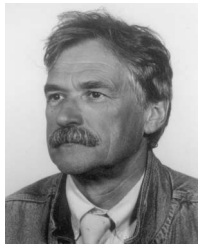

Adriaan A. Van de Griend received the Ph.D. degree in hydrology from Vrije Universiteit (VU) Amsterdam, Amsterdam, The Netherlands.

He retired as an Associate Professor of remote sensing and hydrology from the Department of Hydrology and Geo-Environmental Sciences, VU Amsterdam. His continued research interest lies in remote sensing for hydrology-related applications, particularly in the thermal microwave wavelength bands, with a focus on the effects of spatial heterogeneity and consequences for physical model inversion of signatures gathered from space.